Self-consistent calculations of the electronic structure for ideal Ga and As vacancies in GaAs

Giovanni B. Bachelet, G. A. Baraff, and M. Schlüter
Bell Laboratories, Murray Hill, New Jersey 07974
(Received 18 November 1980; revised manuscript received 25 March 1981).

Self-consistent calculations for both types of vacancies in a polar semiconductor are presented. The study is carried out by the Green's-function method proposed by Baraff and Schlüter and applied to the silicon vacancy. The GaAs band structure was obtained by a self-consistent pseudopotential calculation based on localized orbitals only. The Green's function for the perfect crystal was then expanded in the same basis set, and both vacancies were separately studied. Owing to the polar nature of the host semiconductor, the self-consistent treatment was necessary to obtain reliable results. The Ga vacancy has a very weakly bound state almost degenerate with the top of the valence band, while the As vacancy has a deep bound-state level, 1.08 eV above the top of the valence band. The As vacancy also gives rise to an overall modification of the density of states very similar to the case of the ideal silicon vacancy. Modifications of these results due to lattice-relaxation effects are discussed in light of available experimental data.

I. INTRODUCTION

The electronic structure of localized defects in III–V compounds is of crucial interest in the understanding of optical and electrical properties of a class of materials of major importance in most fields of pure and applied solid-state physics. To study these defects we have adopted the self-consistent approach based on the Green's-function method which was successfully tested in the case of the silicon vacancy.[1]

The study of the two *ideal* neutral vacancies in GaAs is both necessary and useful, because it is required for further calculations involving lattice relaxations around them and already allows an interesting comparison between compound and elemental semiconductors, i.e., the ideal neutral Si vacancy which was previously studied.[1,2] Also, the results for neutral ideal vacancies are the only ones available from other non-self consistent[3–5] or cluster-type[6] calculations. This comparison then allows us to have a direct insight into the specific effects of self-consistency on calculated energies.

In Sec. II we recall the method of calculation; in Sec. III after some general observations on vacancies in compound semiconductors we examine in detail the results obtained for both types of vacancies. Sec. IV is devoted to some conclusions.

II. METHOD OF CALCULATION

We here briefly recall the Green's-function method adopted to the calculation of localized defect states. A point defect is represented by a potential $U(r)$ which vanishes at large distance, and is described by

$$(H_0 + U)\psi(r) = E\psi(r) \ , \tag{1}$$

where $H_0 = -\frac{1}{2}\nabla^2 + V_c$ is the unperturbed Hamiltonian. The defect potential U is the difference between the total self-consistent potentials for the imperfect crystal and the perfect crystal. The physical approximation we use is a one-electron potential, consisting of a local pseudopotential that takes into account the interaction between the ionic cores and the valence electrons, and a Coulomb potential plus a local-exchange–correlation function of the valence electron density to describe the interaction between valence electrons. For the ion pseudopotentials of Ga and As we consistently use the Hamann-Schlüter-Chiang[7]-type pseudopotentials for both band-structure and vacancy calculations. These intrinsically nonlocal pseudopotentials are here approximated by the local $l = 0$ s pseudopotential. This approximation is justified by considering that for both Ga and As the nonlocality (defined as the difference between the s and p pseudopoten-

tials) is small compared to the angular momentum barrier of $l(l+1)/r^2$ effectively experienced by the p electrons. The pseudopotentials, originally obtained in numerical form,[7] were fitted to a superposition of Gaussians plus an error function which describes the Coulomb potential arising from a smeared Gaussian ionic charge:

$$V(r) = -\frac{Z}{r}\,\mathrm{erf}(r\alpha_0^{1/2}) + \sum_i v_i e^{-\alpha_i r^2} \quad . \tag{2}$$

The v_i and α_i were obtained through a least-squares fit. The chosen fits were able to reproduce within 1% the atomic eigenvalues and eigenfunctions of the original nonlocal psuedopotentials (see Table I).

The form of Slater-type exchange and correlation potential $X\alpha$, with $\alpha = 0.79$, was the same for both band-structure and vacancy calculations. The Coulomb potential is obtained by solving Poisson's equation as explained in detail for the silicon-vacancy calculation.[1]

The loop of self-consistency is entered with a starting defect potential obtained by adding an *ad hoc* screening to the unscreened defect (in the language of pseudopotentials and in the case of vacancies, this is the ionic pseudopotential of the missing atom with the opposite sign) and the resulting charge density is evaluated. This charge density is used to calculate a new defect potential, a portion of which is blended to the old starting potential. The process is repeated until input and output potentials agree to within some specified limit at all points in space. The whole process was carried out twice: once for the gallium vacancy, and once for the arsenic vacancy.

TABLE I. Characteristic parameters used for the fit of the pseudopotentials of Ref. 10 to a sum of Gaussians plus an error function times $-Z/r$ according to Eq. (2). Energy in hartrees.

	v_i(a.u.)	α_1(a.u.)$^{-2}$
Ga	−9.89	0.8
$\alpha_0 = 1$	34.3	1.2
	−21.44	1.6
As	8.426	0.727
	−43.46	1.024
$\alpha_0 = 1$	96.57	1.515
	−66.24	2.006
	9.78	2.501

for the arsenic vacancy.

The GaAs band structure was calculated following the approximations cited above, using orbitals of the form

$$\Phi_{lm\alpha}(\vec{r}) = Y_{lm}(\vec{\Omega})r^l e^{-\alpha r^2} \quad ,$$

where $Y_{lm}(\vec{\Omega})$ are spherical harmonics. We took 20 orbitals per atom, i.e., two sets of 9 orbitals

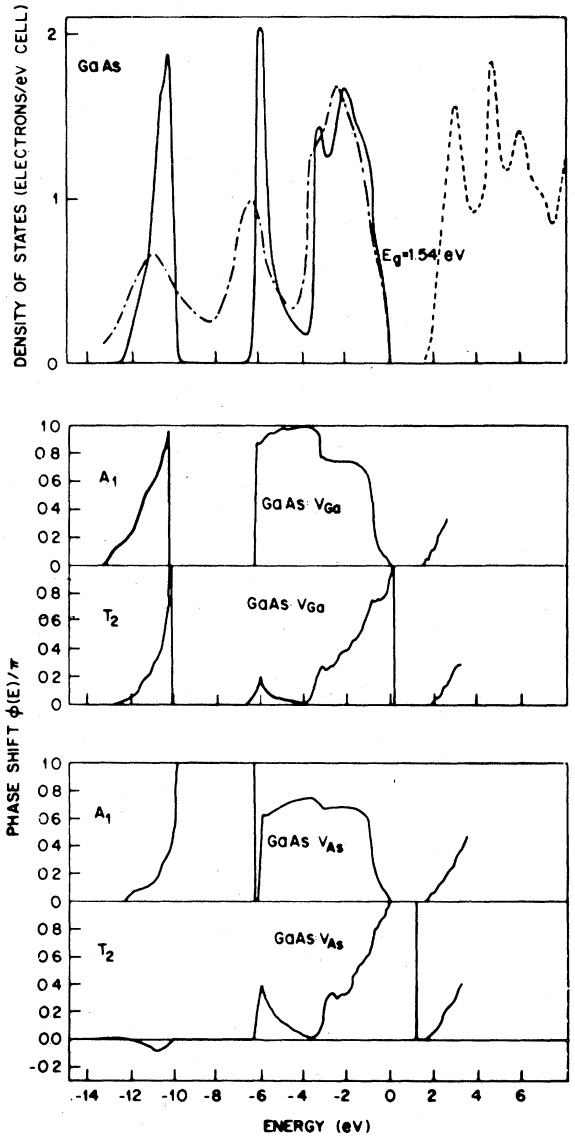

FIG. 1. Top panel: density of states of perfect GaAs for valence (solid line) and conduction (dashed line) bands as obtained in this work and (dash-dotted line) experimentally in Ref. 8. Central and bottom panels: phase shifts induced by a neutral Ga vacancy and by a neutral As vacancy, respectively.

($l = 0,1,2$) plus an additional s function $r^2e^{-\alpha r^2}$, and two decay constants, α_1 and α_2. The choice of $\alpha_1 = 0.2$(a.u.), $\alpha_2 = 0.6$(a.u.) for both Ga and As sites was found to be a convenient one.

The self-consistent band-structure calculation was carried out keeping Hamiltonian and overlap matrix elements up to fifth neighbors. The resulting density of states appears in the top part of Fig. 1. In spite of using a local-exchange–correlation potential the fundamental gap is closer to the experimental value than previous experience with first-principles pseudopotentials would have led one to expect (i.e., too small a gap). This may be the price we pay for the use of a local pseudopotential instead of the full nonlocal first-principles pseudopotential. Since, however, the shape of the density of states is in good agreement with both experimental (dash-dotted line in top Fig. 1: Ref. 8) and previously calculated[12] density of states for GaAs, it is clear that the band structure we obtained is actually meeting the requirements for an appropriate construction of the Green's function for the perfect crystal (see Table II). As in the case of silicon, we evaluate the wave functions on a grid of 70 points per $\frac{1}{48}$ of the Brillouin zone (BZ) and the energies on a grid of 203 points per $\frac{1}{48}$ of BZ. In the expansion of the Green's function it is sufficient to use orbitals out as far as second-nearest neighbors, 17 sites in all. This leads to a total of 340 orbitals, and the largest size of the density matrix, that for representation T_2, is 52×52.

We have taken the same 20 orbitals per atom for calculation of the As and Ga vacancies. (In the language of Ref. 1, inner-set and outer-set orbitals are the same in this calculation.) In Figs. 2 and 3 we see the spherical average of the final self-consistent defect potentials for the As and Ga vacancies, respectively. From the range of these potentials it follows that the choice of extending the inner set to nearest neighbors only is a good approximation. We are thus left with 4 sites and 20 orbitals per site, i.e., 80 orbitals altogether. The maximum size of the matrix $[N - D(E)]$ to be inverted, that for representation T_2, is only 14×14.

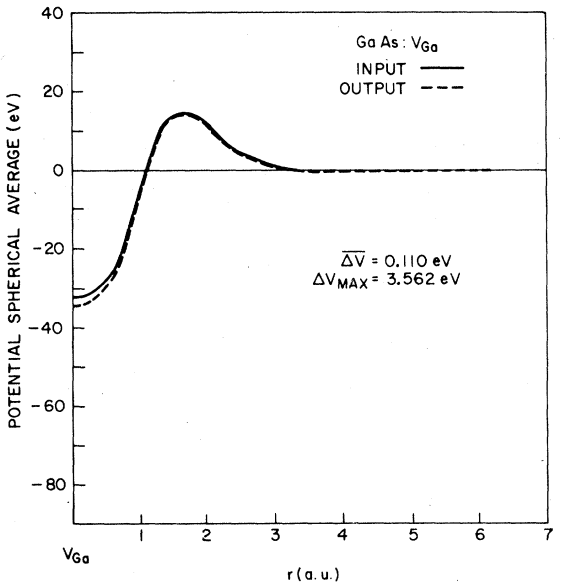

FIG. 2. Spherical average of the self-consistent potential of the gallium vacancy in GaAs for the last iteration. Solid line: input potential; dashed line: output potential.

III. STRUCTURE OF THE VACANCIES IN BINARY ZINC-BLENDE SEMICONDUCTORS

The *ideal* Ga and As vacancies are the first models to be studied before the surrounding lattice

TABLE II. Comparison of energies $E_n(k)$at symmetry points Γ, X, and L obtained in the present work and in Ref. 12. Energy in eV.

Γ	Γ [Ref. (12)]	X	X [Ref. (12)]	L	L [Ref. (12)]
−12.28	−12.55	−10.15	−9.83	−10.80	−10.60
0.00	−0.35	−6.27	−6.88	−6.08	−6.83
	0.00				
1.54	1.51	−2.33	−2.99	−0.95	−1.42
			−2.89		−1.20
3.92	4.55	1.95	2.03	1.67	1.82
	4.71	2.16	2.38	4.73	5.52

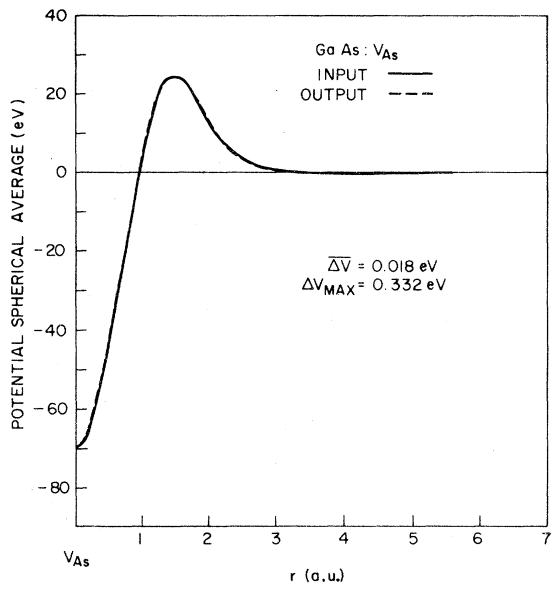

FIG. 3. Spherical average of the self-consistent potential of the arsenic vacancy in GaAs for the last iteration.

is allowed to relax. Furthermore, it is interesting to compare the results of this self-consistent calculation for vacancies in polar semiconductors to the purely covalent case, to infer trends in the behavior upon lattice relaxations.[10,17]

An ideal A vacancy in a binary semiconductor $A^M B^N$ ($M + N = 8$) with zinc-blende structure is surrounded by 4 B atoms that remain in their bulk crystalline positions, and its creation results in four broken bonds pointing from the 4 B atoms towards the A vacancy. The *neutral* A vacancy is created by removing the A^{M+} ion and M electrons, while for a B vacancy (surrounded by 4 A atoms) the B^{N+} ion and N electrons are removed. Thus the four neighbors are of different chemical species for A and B vacancies, as are the number of electrons to be removed together with the missing ions. Various experimental results[10–15] indicate that the two types of vacancies in compound zinc-blende semiconductors indeed behave in different ways. Moreover, the removal of neutral atoms modifies the somewhat ionic character, present in the perfect $A^M B^N$ crystal. As a result, the *self-consistent* potential experienced by the electrons in the neighboring atoms is expected to be different from that obtained by the simple atom-removal procedure which applied quite well to the covalent Si case. Thus for polar semiconductors self-consistency is expected to modify the results of non-self-consistent calculations based on empirical tight-binding parameters.[5] Note that, in addition to change self-consistency effects, empirical tight-binding calculations are often affected by an insufficient description of the crystal conduction bands.[16]

However, both the symmetry classification of the different contributions to the change in the density of states and the simple physical picture of their meaning in terms of the broken bonds remain unchanged for the Ga and As vacancies in GaAs, and we refer to the discussion of the Si vacancy.[1] We just recall that T_d, the point group of the vacancy, has five representations $\Gamma_1(A_1)$, Γ_2, Γ_3,Γ_4, Γ_5, (T_2), the first one-dimensional, the third two-dimensional, and the fourth and fifth three-dimensional. The A_1 and T_2 representations may be seen, in terms of the four broken bonds a, b, c, and d, as the nodeless, totally symmetric combination $a + b + c + d$ (s character at the vacancy site) and the three degenerate combinations of the type $a + b - c - d$ (p character at the vacancy site), respectively. The Γ_3 and Γ_4 representations involve back bonds only and are expected to give very small contributions to the total change in the density of states.

A. Gallium vacancy

In Fig. 1 (top) we display the bulk density of states as obtained in our self-consistent band-structure calculation. In the central panel the A_1 and T_2 phase shifts induced by the self-consistent Ga vacancy potential are shown on the same energy scale. The phase shifts $\phi(E)$ have been calculated according to Ref. 1 and describe the energy distribution of changes induced in the density of states $\Delta n(E)$: The integral

$$\int_{E_1}^{E_2} \Delta n(E) = -\frac{1}{\pi}[\phi(E_2) - \phi(E_1)] \qquad (3)$$

shows that the number of states gained (or lost) in the energy interval $E_1 < E < E_2$ is equal to π^{-1} times the difference in the phase shifts at the limits of the interval. Since the imaginary part of the Green's function vanishes in the gaps, the phase shift there must be a multiple of π, and the edge-to-edge integral over a band must produce an integer number of lost or gained states. This is separately true for the contributions of different symmetry types. Thus the interpretation of the lower panels of Fig. 1 is straightforward. Looking at the central panel we see that for the A_1 symmetry the ideal neutral Ga vacancy has neither gained nor lost states from its valence band, but a strong resonance shows up at the upper edge of the lower gap and

TABLE III. A_1 and T_2 levels and $T_2 - A_1$ splittings for V_{Ga} and V_{As} (the energy zero is at the top of the valence band) as obtained in different calculations. *A*: imperfect-crystal method Ref. 4; *B*: empirical tight binding Ref. 5; *C*: self-consistent $X\alpha$ cluster Ref. 6 ; *D*: present work. Energy in eV.

	A			*B*			*C*			*D*		
	A_1	T_2	$T_2 - A_1$	A_1	T_2	$T_2 - A_1$	A_1	T_2	$T_2 - A_1$	A_1	T_2	$T_2 - A_1$
V_{Ga}	0.2	0.3	0.10	−0.6	0.02	0.62	−0.98	0.55	1.53	−1.0	0.06	1.06
V_{As}	1.18	1.25	0.07	0.71	1.47	0.76	0.86	1.33	0.47	−0.8	1.08	1.88

another appears 1 eV below the top of the valence band with a width of ± 0.4 eV. For the T_2 symmetry, one threefold-degenerate state is lost through a strong antiresonance at the upper edge of the lower gap and another one is lost at the top of the valence band. Both are immediately recovered as true bound states very close in energy to the corresponding edges. The binding energy of the T_2 bound state in the fundamental gap is 0.06 eV and the energy of the lower bound state is at -10.05 eV, 0.1 eV above the edge of the lowest band.

In the upper half of Table III we compare for the Ga vacancy the position of the A_1 resonance and T_2 bound state in the fundamental gap region to the same levels previously calculated by the imperfect-crystal method,[4] the empirical tight-binding method,[5] and by self-consistent cluster calculations.[6] The $A_1 - T_2$ splitting is also displayed. We notice that, for the case of the Ga vacancy, the empirical tight-binding calculations yield overall results compatible with our self-consistent results. However, the A_1 resonance is lowered and thus the $A_1 - T_2$ splitting is increased by self-consistency. On the other hand, the cluster calculations for the Ga vacancy yield levels that are not compatible with either method. Looking at the nature of our self-consistent T_2 bound states at $E = 0.06$ eV we notice that the gap bound state of V_{Ga} is almost degenerate with the band edge (i.e., with a continuum of extended states). Thus, both the chosen size for the cluster and the intrinsic lack of connection to Bloch states of the perfect crystal seem to prevent a proper description of the gallium vacancy in a cluster approach.

Figures 4 and 5 show the A_1 and T_2 changes in the density of states for the Ga vacancy as obtained by this work and in Ref. 5, respectively. The overall agreement between the two figures suggests that the tight-binding method gives a good approximation to the physics of the Ga vacancy. More detailed comparison shows that the A_1 resonance at the top of the valence band has been lowered by self-consistency. The lower A_1 resonance in Fig. 11 has been found as a very loosely bound state in Ref. 5 and thus does not appear in Fig. 5; but the energy difference is of the same order of magnitude as the relative precision in two different band-structure calculations. The shape of the T_2 curves is similar up to -1 eV, where, due to the presence of a loosely T_2 bound state in the fundamental gap, one would expect an antiresonance in both cases; instead, the tight-binding results of Ref. 5 show only a pronounced resonance presumably merging with the bound-state at 0.02 eV. The position of both the

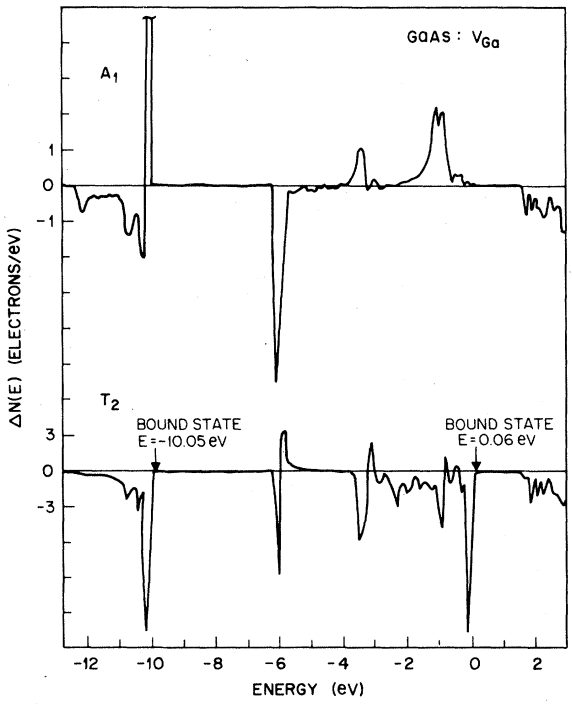

FIG. 4. A_1 and T_2 contributions to the change in density of states induced by an isolated neutral Ga vacancy in GaAs as obtained in this work.

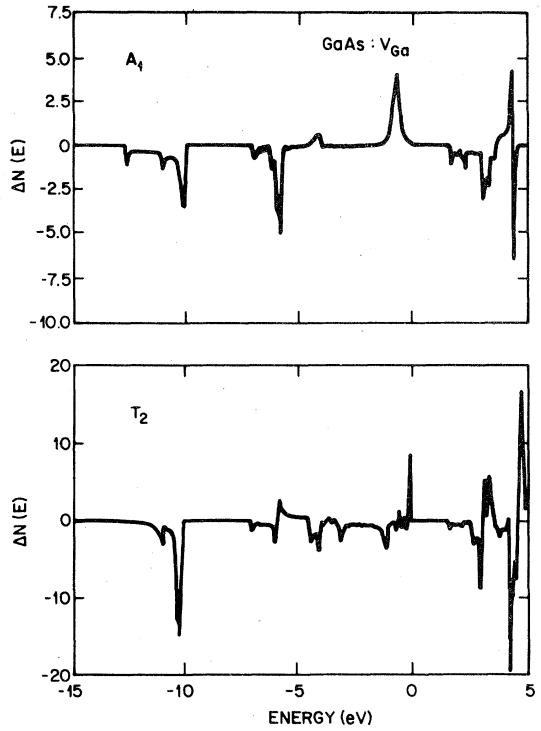

FIG. 5. A_1 and T_2 contributions to the change in the density of states induced by an isolated neutral Ga vacancy in GaAs as obtained in an empirical tight-binding calculation (Ref. 5).

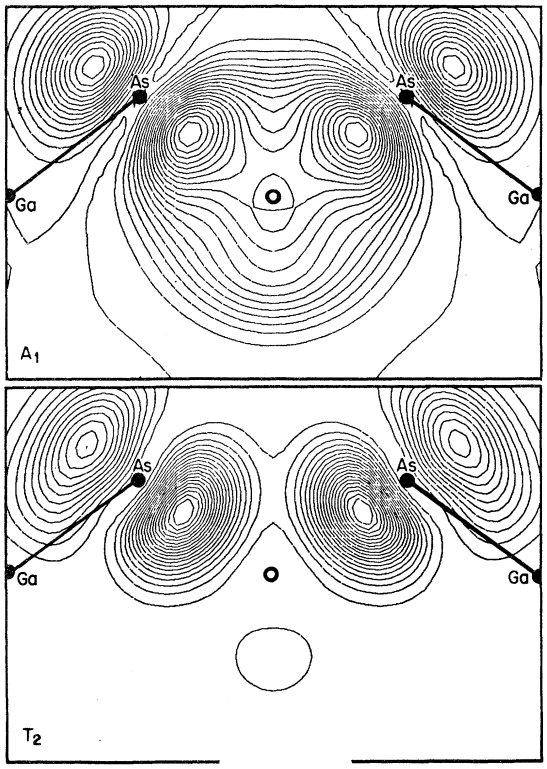

FIG. 6. Charge-density contour plots displayed in a (110) plane of atoms containing one Ga vacancy. The charge density associated to the A_1 resonance at -1.0 eV (top) and to the T_2 loosely bound state at 0.06 eV (bottom) are shown. Units can be deduced from the corresponding bond profiles in top of Fig. 7.

lower and the upper T_2 bound states, not displayed in the figures, is almost identical for both calculations (see Table III).

Our results for the ideal Ga vacancy could not be carried to full self-consistency (Fig. 2) because of the tendency of the partially filled T_2 level to dip into the top of the valence bands. This instability is, of course, somewhat artifical since lattice distortions of either the Jahn-Teller type or the symmetric breathing type are expected to occur, which will alter the level structure.

The correlation between the structure in the phase shifts and the structure in the density of states of the perfect crystal, which had been found and emphasized in previous papers concerning vacancies in covalent semiconductors,[1,17] appears clearly in the case of both types of vacancies for this example of a polar semiconductor, and the arguments previously pointed out apply here as well.

The charge density associated with the A_1 resonance at -1 eV and with the T_2 bound state at 0.06 eV are displayed as contours in the (110) plane containing two dangling bonds and the Ga vacancy (Fig. 6). The charges are also shown as profiles along the direction of the dangling bonds (Fig. 7, top). Both states are close to the top of the valence band and clearly appear as combinations of mainly *p*-like orbitals of the neighboring As atoms. Comparison to the bond profiles shows that both states give positive contributions to the total charge disturbance. Analyzing the A_1 phase shifts in detail we find that the antiresonance at the onset of the valence band and the strong resonance following it appear both as combinations of mainly *s*-like arsenic orbitals, but the two charge contributions have *opposite* signs and their sum, whose integrated net charge is zero, results in a charge transfer from the vacancy site to the back bonds. This is a consequence of charge rearrangement upon having removed a neutral Ga atom from slightly ionic crystalline environment. Similarly, for T_2 symmetry charge transfer occurs from the vacancy site to the back bonds. This charge transfer originates from an antireso-

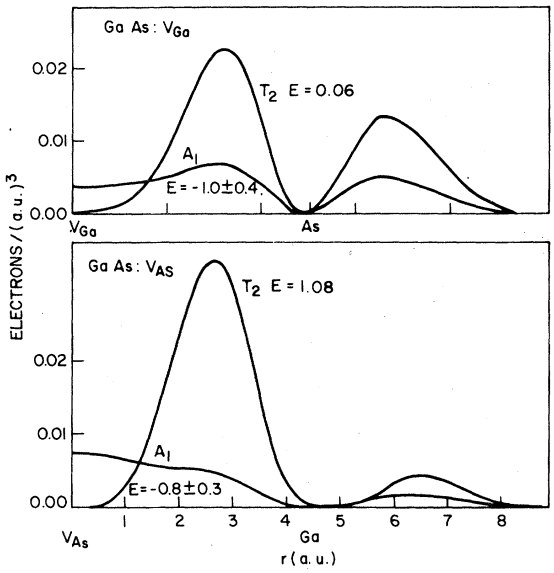

FIG. 7. Charge-density profiles associated with the A_1 resonance (-1.0 eV) and the T_2 bound state (0.06 eV) of the Ga vacancy (top) and with the A_1 resonance (-0.8 eV) and the T_2 bound state (1.08 eV) of the As vacancy (bottom) plotted along the direction of the broken bond (compare top with Fig. 6 and bottom with Fig. 13).

nance at the onset of the valence band closely followed by loosely bound state $E = -10.05$ eV.

The sum of the scattering-state charge densities from all symmetries contains also the small Γ_3 and Γ_4 contributions, whose phase shifts, although not displayed, are part of the calculation. In contrast, no Γ_2 contributions arise in our approximation because the nearest orbitals that could give rise to a Γ_2 phase shift (p and d orbitals centered at the second-nearest neighbors) are not included in our inner LCAO set.

The total charge disturbance is produced as the superposition of all scattering states and the bound states are appropriately occupied. In our case, to yield charge neutrality we fill the higher T_2 bound state to one-half occupancy. We see that the main part of the total charge disturbance ($\Delta\rho$ in Figs. 8 and 9) is of a much shorter range than the individual bound states and resonances (Figs. 6 and 7 top). This is a common observation for self-consistent calculations concerning defects and surfaces in solids.[1,2,18,19] This physical effect allows us to face the problem of self-consistency using the Green's-function method with a reasonable number of orbitals and neighbors. In contrast to covalent silicon, however, some small longer range charge fluctuations persist due to the partial ionic nature of GaAs.

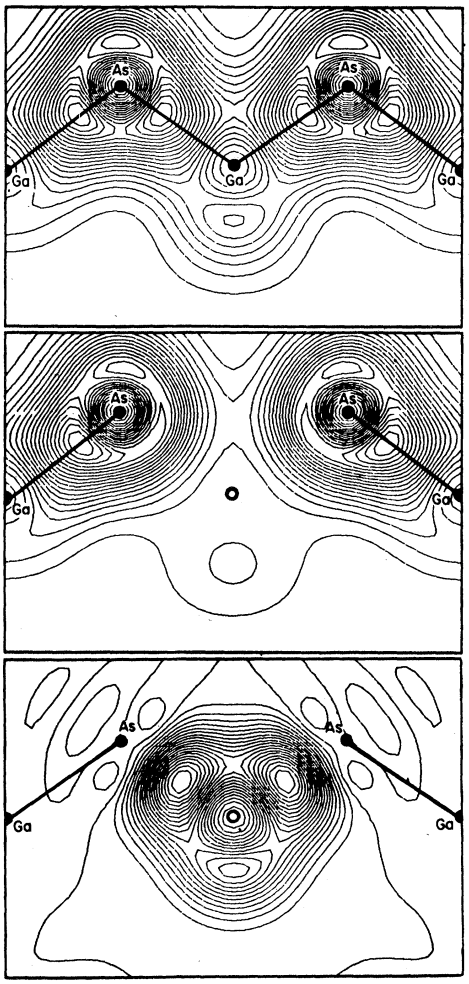

FIG. 8. Charge contour plots along the (110) plane for the Ga vacancy. Top: unperturbed GaAs. Center: GaAs with one Ga vacancy. Bottom: total charge disturbance introduced by the Ga vacancy. Units can be deduced from the corresponding profiles in Fig. 12.

The perturbed charge density ρ in Figs. 8 and 9 shows the disappearance of the bonding charge with the removal of the gallium atom.

B. Arsenic vacancy

In the case of the arsenic vacancy the overall structure of the phase shifts is quite similar to the case of the silicon vacancy, as can be seen in Fig. 1 (bottom panel). Quantitatively, differences occur. In contrast to the case of Si, the A_1 antiresonance corresponding to the onset of the valence band is so strong for As vacancies that a complete state, i.e., the As s state, is removed.

Near the fundamental gap a sharp A_1 resonance

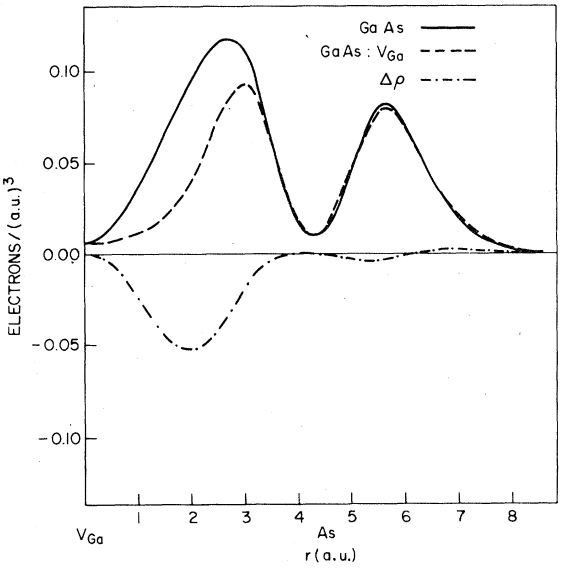

FIG. 9. Charge-density profiles along the direction of the broken bond. Solid line: unperturbed GaAs. Dashed line: GaAs with one Ga vacancy. Dash-dotted line: total charge disturbance introduced by the Ga vacancy.

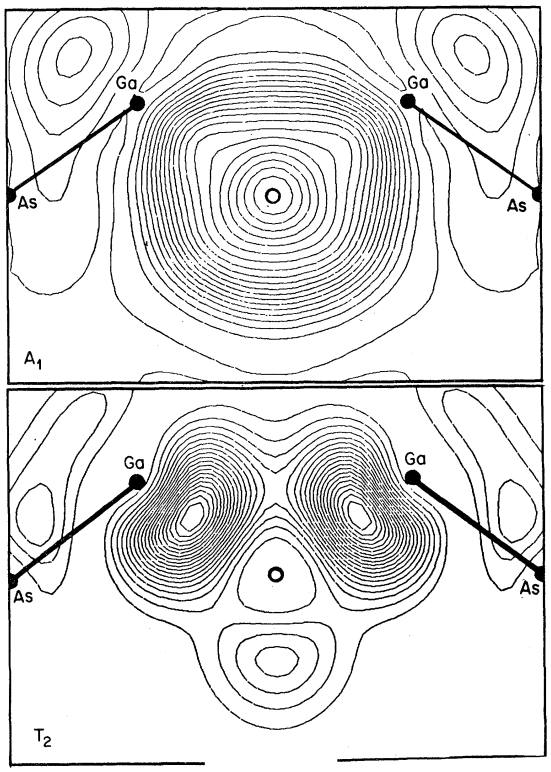

FIG. 10. Charge-density contour plots displayed in a (110) plane of atoms containing one As vacancy. Top: charge density associated with the A_1 resonance at -0.8 eV. Bottom: charge density associated with the T_2 bound state at 1.08 eV. Units can be deduced from the corresponding bond profiles in bottom Fig. 7.

if found at -0.8 ± 0.3 eV and a T_2 bound state appears at 1.08 eV. Thus a deep level is associated with the ideal arsenic vacancy. The corresponding charge densities are shown in Fig. 7 (bottom) and in Fig. 10. We see that the A_1 resonance and especially the T_2 bound state are much more localized than in the case of the gallium vacancy, and practically all the charge lies in the region of the dangling bonds.

The position of the T_2 bound state is well separated from both band edges at about $\frac{2}{3}$ of the fundamental gap and full self-consistency could be achieved [i.e., input and output potentials agreed on the average to 0.02 eV with a maximum of 0.33 eV (Fig. 3)]. The T_2 bound state (Figs. 7 and 10) is filled to one-sixth occupancy to yield a charge-neutral vacancy. We look again at Table III to compare the position of the A_1 and T_2 levels in the gap region with the results of previous calculations. The position of the T_2 bound state is roughly compatible among all calculations, but again we see that self-consistency has radically lowered the position of the A_1 level and increased the $A_1 - T_2$ splitting.

In Figs. 11 and 12 we compare our changes in the density of states obtained for the As vacancy to the tight-binding results of Ref. 5. More pronounced differences than in the case of the Ga vacancy occur, in particular, for the A_1 contributions. The strong A_1 resonances at -0.8 eV is found in Ref. 5 as a true bound state well inside the gap with $E = 0.71$ eV. As a consequence the whole structure above the lower gap looks quite different; only the antiresonance at the bottom of the lower gap is almost identical in the two cases. On the other hand, the T_2 symmetry shows similar changes in the density of states for both calculations. The effect of self-consistency can also be seen for the case of both vacancies in Table IV, where we monitor the positions of the A_1 and T_2 levels in the gap region as a function of iterations.

We now look in more detail at the phase shifts of the As vacancy and the corresponding charge contributions. The density of states of the perfect crystal loses a state of A_1 symmetry at the onset of the valence band, i.e., an arsenic s-like state. A bound state, very close to the upper edge of the lower gap at $E = -6.37$ eV is followed by an antiresonance. In contrast to the Ga vacancy the bound-state antiresonance pair corresponds to moving charge away from the back bonds into the vacancy region. This

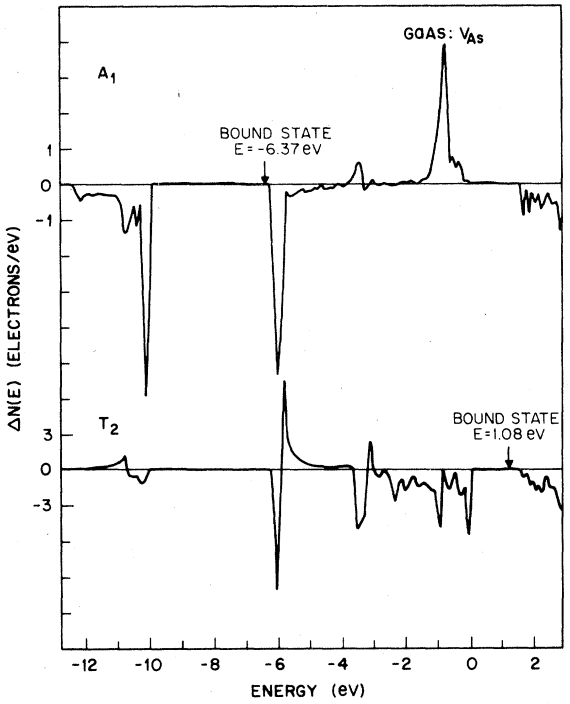

FIG. 11. A_1 and T_2 contributions to the change in the density of states induced by an isolated neutral As vacancy in GaAs as obtained in this work.

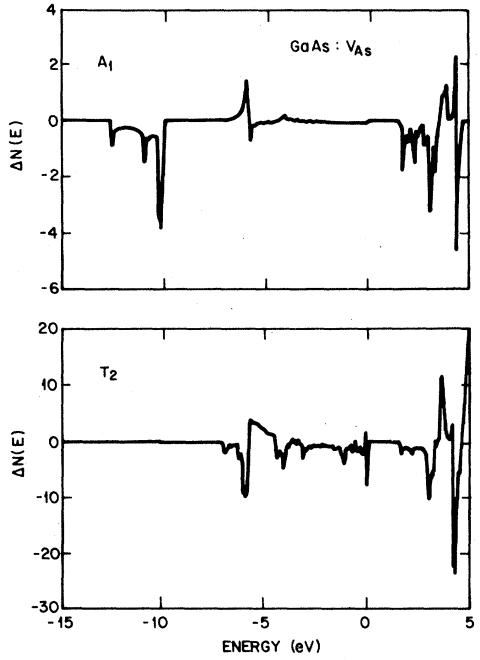

FIG. 12. A_1 and T_2 contributions to the change in the density of states induced by an isolated neutral As vacancy in GaAs as obtained in an empirical tight-binding calculation (Ref. 5). Units can also be deduced from Fig. 6.

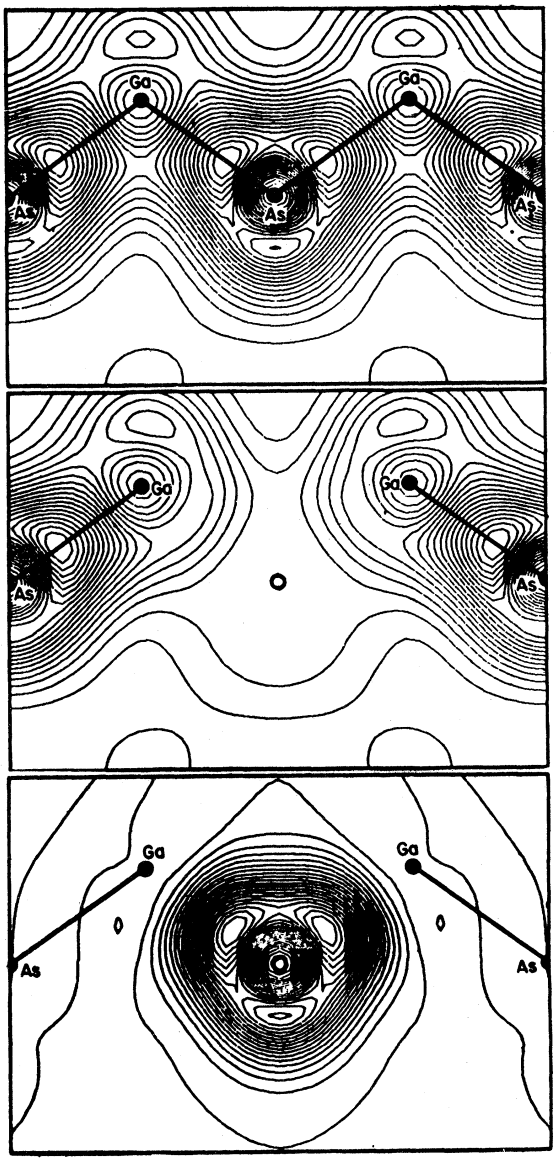

FIG. 13. Charge contour plots along the (110) plane for the As vacancy. Top: unperturbed GaAs. Center: GaAs with one As vacancy. Bottom: total charge disturbance introduced by the As vacancy. Units can be deduced from the corresponding bond profiles in Fig. 12.

is a consequence of having removed a neutral As atom from a slightly ionic crystalline environment. The total contribution of the scattering states shows a charge which is more localized in the dangling-bond region than it was in the case of the neutral gallium vacancy.

Finally we look at the total unperturbed and perturbed charge density, and at the difference charge

TABLE IV. Position of the A_1, T_2 levels and the $T_2 - A_1$ splitting as a function of the iterations performed before reaching self-consistency. Energy in eV.

		1	2	3	4	5	6	7	8	9	10
V_{Ga}	A_1	0.0	−0.7	−0.8	−0.9	−1.0	−1.1	−1.0			
	T_2	0.8	0.15	0.2	0.18	0.08	0.03	0.06			
	$T_2 - A_1$	0.8	0.85	1.0	1.08	1.08	1.13	1.06			
V_{As}	A_1	1.4	0.98	−0.3	−1.0	−1.3	−1.1	−0.7	−0.9	−0.8	−0.8
	T_2	2.2	2.1	1.51	1.08	0.97	0.88	1.28	1.16	0.96	1.08
	$T_2 - A_1$	0.8	1.12	1.81	2.08	2.27	1.98	1.98	2.06	1.76	1.88

perturbance introduced by the arsenic vacancy (Figs. 13 and 14). Comparing ρ and $\Delta\rho$ with the previous case of the gallium vacancy (Figs. 8 and 9) we notice that the total charge perturbance of the arsenic vacancy is both larger and more localized. This is expected, since the As vacancy corresponds to the presence of a more repulsive potential plus the removal of five electrons in the environment of less attractive Ga potentials. In the case of the Ga vacancy, on the other hand, a more shallow repulsive potential was surrounded by more attractive As potentials and three electrons only had to be removed. This explains very well why in the case of gallium the charge perturbance is still slightly different from zero at two bond lengths away from the vacancy (Fig. 9).

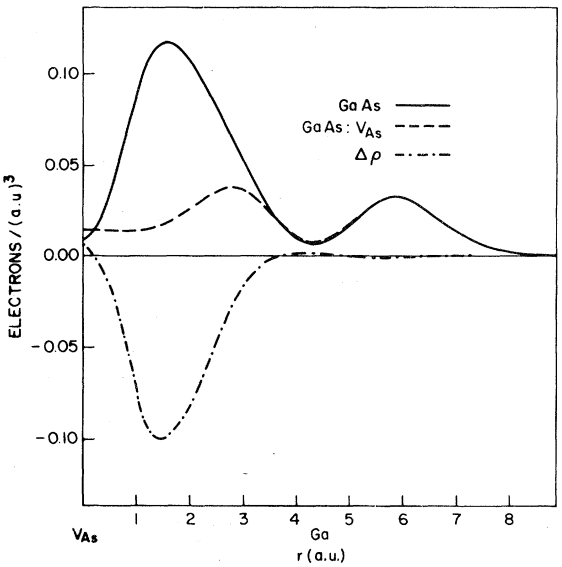

FIG. 14. Charge-density profiles along the direction of the broken bond. Solid line: unperturbed GaAs. Dashed line: GaAs with one As vacancy. Dash-dotted line: total charge disturbance introduced by the As vacancy.

IV. CONCLUSION

We calculated with the self-consistent Green's-function technique the electronic structure of the ideal neutral Ga and As vacancies in GaAs. We obtained in the gap region a bound state at $E = 1.08$ eV, i.e., almost degenerate with the top of the valence band for the Ga vacancy. It is tempting to conclude that the As vacancy is the more important defect of the two vacancies in GaAs on the ground of the deep-level energies. This may, however, not be correct. In fact, observed trends in elemental and compound II−VI semiconductors[10] show that the metal vacancy in compound materials exhibits large Jahn-Teller distortions. More recent observations[14] confirm that the Ga vacancy is indeed responsible for one of the deep levels related to simple native defect of GaAs. General trends[10] together with experimental evidence[14] tell us that our results, obtained for the neutral ideal Ga vacancy, are expected to be strongly modified by Jahn-Teller distortions, and that only after the different charge states of the relaxed vacancy have been calculated, transitions between the appropriate configurations can be reasonably compared to the experimental results. In particular, available DLTS (deep-level transient spectroscopy) data[14] referring to n-doped samples show a deep $E3$ line which is attributed to the Ga vacancy. We believe that this signal could arise, for instance, from a $V^- \rightarrow V^0$ transition, after the ideal V^0 level has been split by Jahn-Teller distortions into two levels, one below and one above the valence-band edge.

On the other hand, the energetic position of the T_2 state of the ideal neutral As vacancy in the gap suggests that the relaxed As vacancy could still be a deep level and thus has to be associated to another observed deep level in GaAs, whose nature has not yet been fully understood. The As vacancy also seems to play an important role in the luminescence lines of GaAs (Refs. 12 and 13), but in this case its role is often described in terms of more complicated complexes (like a hold loosely bound to a $Si_{Ga} - V_{As}$ complex[13]).

Finally, the overall shape of the modifications of the density of states of the infinite crystal induced by the ideal As vacancy closely resembles that of the ideal silicon vacancy. This suggests also that its behavior upon relaxation may resemble that of Si and may also exhibit "Anderson negative-U" character.[20]

[1]G. A. Baraff and M. Schlüter, Phys. Rev. Lett. 41, 892 (1978); G. A. Baraff and M. Schlüter, Phys. Rev. B 19, 4965 (1979).

[2]J. Bernholc, N. Lipari, and S. T. Pantelides, Phys. Rev. Lett. 41, 895 (1978); J. Bernholc, N. O. Lipari, and S. T. Pantelides, Phys. Rev. B 21, 3545 (1980).

[3]M. Jaros and S. Brand, Phys. Rev. B 14, 4724 (1976).

[4]N. P. Il'in and V. F. Masterov, Fiz. Tekh. Poluprovodn. 10, 436 (1976) [Sov. Phys.—Semicond. 10, 496 (1976)].

[5]J. Bernholc and S. T. Pantelides, Phys. Rev. B 18, 1780 (1978).

[6]A. Fazzio, J. R. Leite, and M. L. DeSigueria, J. Phys. C 11, 1001 (1978); J. Phys. C 12, 3469 (1979).

[7]D. R. Hamann, M. Schlüter, and C. Chiang, Phys. Rev. Lett. 43, 1494 (1979).

[8]L. Ley, R. A. Pollak, F. R. McFeely, S. P. Kowalczyk, and D. A. Shirley, Phys. Rev. B 9, 600 (1974).

[9]M. S. Liu, K. Gamo, K. Masuda, S. Namba, Jpn. J. Appl. Phys. 14, 1839 (1975).

[10]G. D. Watkins, in *Radiation Damage and Defects in Semiconductors, 1972* (Institute of Physics, London, 1973), p. 228.

[11]S. Y. Chiang and G. L. Pearson, J. Appl. Phys. 46, 2986 (1975).

[12]J. R. Chelikowsky and Marvin L. Cohen, Phys. Rev. B 14, 556 (1976).

[13]T. Itoh and M. Takeuchi, Jpn. Appl. Phys. 16, 227 (1977).

[14]D. V. Lang, R. A. Logan, and L. C. Kimerling, Phys. Rev. B 15, 4874 (1977); D. V. Lang, in *Radiation Effects in Semiconductors, Dubrovnik, 1976,* edited by N. B. Urli and J. W. Corbett (Institute of Physics, London, 1977), p. 70.

[15]H. Kasano, J. Appl. Phys. 49, 4746 (1978).

[16]D. A. Papaconstantopoulos and E. N. Economou, Phys. Rev. B 22, 2903 (1980).

[17]J. Callaway, J. Math. Phys. 5, 783 (1964); J. Callaway and A. J. Hughes, Phys. Rev. 156, 860 (1967); J. Callaway, Phys. Rev. B 3, 2556 (1971); F. P. Larkins and A. M. Stoneham, J. Phys. C 4, 143 (1971); E. Kauffer, P. Pecheur, and M. Gere, *ibid.* 9, 2319 (1976); William Y. Hsu *et al.*, Phys. Rev. B 16, 1597 (1977); J. D. Joannopoulos and Eugene J. Mele, Solid State Commun. 20, 729 (1976); M. Lannoo and P. Lenglart, J. Phys. Chem. Solids 30, 2409 (1969); and Refs. 1 and 2.

[18]J. R. Appelbaum and D. R. Hamann, Rev. Mod. Phys. 48, 479 (1976).

[19]M. Schlüter, J. R. Chelikowsky, S. G. Louie, and Marvin L. Cohen, Phys. Rev. B 12, 4200 (1975).

[20]G. A. Baraff, E. O. Kane, and M. Schlüter, Phys. Rev. Lett. 43, 956 (1979); Phys. Rev. B 21, 3563 (1979); 21, 5662 (1980).